Journal of Histochemistry & Cytochemistry 2018, Vol. 66(8) 563–576

DOI: 10.1369/0022155418768230
journals.sagepub.com/home/jhc
SAGE

Depolarized Hepatocytes Express the Stem/Progenitor Cell Marker Neighbor of Punc E11 After Bile Duct Ligation in Mice

Andrea Bowe*, Susanne Zweerink*, Vera Mück, Vangelis Kondylis, Sigrid Schulte, Tobias Goeser, and Dirk Nierhoff

Department of Gastroenterology and Hepatology, University Hospital of Cologne, Cologne, Germany (AB, SZ, VM, SS, TG, DN); and Institute for Genetics, Centre for Molecular Medicine, Cologne Excellence Cluster on Cellular Stress Responses in Aging-Associated Diseases, University of Cologne, Cologne, Germany (VK)

Summary

There is a medical need of biomarkers for disease stratification in cholestatic liver diseases that come along with changes in hepatocyte polarity. Neighbor of Punc E11 (Nope) is an oncofetal marker that is lost after final differentiation and polarization of hepatocytes. We analyzed the expression pattern of Nope and connexin (Cx) 26 as markers of hepatocyte polarization during murine liver development as well as in adult liver with or without bile duct ligation (BDL) by quantitative real-time reverse transcription polymerase chain reaction (qRT-PCR), western blotting (WB), and immunohistochemistry. Nope is highly expressed in fetal and postnatal liver but barely detectable thereafter. Cx26, however, is much higher expressed in adult than in fetal liver. Postnatally, Nope is directed to the sinusoidal membrane of early hepatocytes while Cx26 remains distributed over the whole membrane indicating limited polarization. In the adult liver, only Cx26 is detectable and restricted to the bile canalicular domain indicating fully polarized hepatocytes. After BDL, Nope is again >300-fold upregulated while Cx26 is reduced rapidly. By immunohistochemistry, Nope identifies a subset of hepatocytes with randomly distributed Cx26. In summary, Nope identifies depolarized adult hepatocytes after cholestatic liver injury resembling early postnatal hepatocytes. Therefore, Nope might be a valuable histochemical biomarker allowing stage-specific stratifications in cholestatic liver diseases. (J Histochem Cytochem 66:563–576, 2018)

Keywords

cholestasis, IGDCC4, mouse

Introduction

Biomarkers have become a highly valuable tool in clinical oncology, as they have proven useful in diagnosis and prognosis as well as in predicting and monitoring of treatment response in various cancers. In cholestatic liver diseases, however, there is an urgent medical need of tools including biomarkers for individual disease stratification that may help to offer stage-specific treatment options[1] and recent evidence shows that cholestatic liver injury comes along with changes in hepatocyte polarity.[2]

Neighbor of Punc E11 (Nope) is an oncofetal stem/progenitor cell marker that was first identified in the liver by microarray analysis of murine fetal liver.[3,4] During liver development, Nope is highly expressed on

Received for publication September 8, 2017; accepted February 28, 2018.

*These authors contributed equally.

Corresponding Author:
Dirk Nierhoff, Department of Gastroenterology and Hepatology, University Hospital of Cologne, Kerpener Str. 62, 50937 Cologne, Germany.
E-mail: dirk.nierhoff@uk-koeln.de

Journal of Histochemistry & Cytochemistry

the plasma membrane of stem/progenitor cells until birth. Postnatally, the expression level of Nope declines rapidly and Nope is specifically directed to the sinusoidal membrane of early hepatocytes until 2 weeks after birth and remains barely detectable thereafter.[5]

This time course parallels the final maturation and polarization of the developing liver which is completed 2 weeks after birth and can also be described via gap junction formation that occurs at the canalicular membrane of hepatocytes enabling intercellular communication.[6] Although early hepatic progenitor cells express connexin (Cx) 43, there is a switch to Cx26 and Cx32 with the beginning of hepatocytic differentiation.[7] In rats, Cx26 and Cx32 show a maximal expression level at 1 week postnatally (wpn)[8] and continuous expression of both proteins is essential for tissue homeostasis.[9,10]

Several studies have shown that markers of hepatocytic polarization are diminished and mislocalized after liver injury and in the following regeneration process[11,12] though a bile canalicular domain identity is conserved throughout the time and resembles the different embryonic stages until junctional complexes are fully matured and able to regain strict domain occlusion.[13] Specifically, Cx26 and Cx32 have been shown to be reduced after bile duct ligation (BDL) in a rat model.[14]

We hypothesized that Nope on the sinusoidal membrane and Cx26 on the bile canalicular domain of hepatocytes are not only useful to describe physiological formation of hepatocyte polarity during liver development but may also help to identify changes in hepatocyte polarity after cholestatic liver injury.

The aim of our study is the evaluation of Nope as a marker of hepatocyte polarity along liver development and after cholestatic liver injury. We therefore analyzed the differential expression pattern of Nope and Cx26 in different settings: We used fetal and postnatal livers to study physiological formation of hepatocyte polarity and isolated adult hepatocytes after perfusion of adult liver (AL) to model loss of polarity. Finally, we made a comparative analysis with the differential expression pattern of Nope and Cx26 in adult liver with or without BDL as a model of cholestatic liver injury.

Materials and Methods

Mice

C57Bl/6 mice were used to conduct in vitro and in vivo experiments as outlined below.

Pregnant C57Bl/6 mice were purchased from Janvier (Le Genest St. Isle, France). Fetal livers were microdissected at different stages of embryonic development starting at embryonic day (ED) 13.5. For analysis of later stages of liver development, livers were dissected 2 days postnatally (dpn) as well as 1 to 6 wpn and from adult animals. Animals were housed in individually ventilated cages in the mouse facility at the Institute of Pharmacology, University of Cologne, kept under a 12-hr light cycle, and given a regular chow diet (Harlan, diet no. 2918) and water ad libitum. Experiments were approved by the State Agency for Nature, Environment and Consumer Protection (LANUV) North Rhine-Westphalia, Recklinghausen, Germany (Protocol No. 84-02.04.2012.A392) and were in accordance with the German Animal Welfare Act as well as the German Regulation for the protection of animals used for experimental purposes or other scientific purposes. The experiments were planned and performed according to the 3Rs concept of reduction, refinement, and replacement.

Bile Duct Ligation

The common bile duct was ligated under general anesthesia (2% isoflurane inhalation, carprofen 4 mg/kg subcutaneously) with two ligatures close to the liver hilum immediately below the bifurcation and one ligature around the cystic duct. Control animals underwent sham operation with preparation but without ligation of the common bile duct. All surgical procedures were performed under sterile conditions. Animals were sacrificed and liver tissue harvested at 1, 2, 3, 5, 7, 14, 21, 28, and 35 days after surgery. For each time point, three mice were analyzed. To validate the efficiency of the ligation, bilirubin levels were measured in the serum of all mice (Supplementary Table 1). In total, 36 bile duct-ligated mice were used for further analysis, two mice with a bilirubin level of <8 mg/dl 5 days after ligation were excluded from further validation.

Hepatocyte Isolation

Primary hepatocytes were isolated from 4- to 6-week-old C57Bl/6 mice as described previously.[15] In brief, anesthetized mice were perfused via the vena cava with solution I (Earle's balanced salt solution [EBSS] without Ca^{2+} and Mg^{2+}, 0.5 mM ethylene glycol-tetraacetic acid [EGTA]). Subsequently, perfusion with 50 ml of collagenase solution—EBSS with Ca^{2+} and Mg^{2+}, 10 mM 4-(2-hydroxyethyl)-1-piperazineethanesulfonic acid (HEPES), 15 mg collagenase type 2 and 2 mg trypsin inhibitor—was performed and single cell suspensions of the perfused liver were generated using a 70-µm nylon mesh filter. Hepatocytes were washed twice in high glucose Dulbecco's modified Eagle medium (DMEM) supplemented with 1.5% fetal calf serum (FCS), penicillin, and streptomycin, followed by

seeding on collagen-coated plates. The medium was renewed 4 hr later to remove any unattached/dying cells and thereafter every 24 hr. RNA was extracted at 1, 4, and 6 days after isolation.

RNA Extraction

Total RNA from primary cell cultures and all specimens was extracted using the NucleoSpin RNA (Macherey-Nagel GmbH & CO.KG, Dueren, Germany) following the instructions of the manufacturer. RNA quantity was estimated using a Nanodrop ND-1000 Spectrophotometer (NanoDrop Technologies, Wilmington, DE).

Quantitative Real-time Reverse Transcription Polymerase Chain Reaction

Differential expression of Nope and Cx26 was analyzed using quantitative real-time reverse transcription polymerase chain reaction (qRT-PCR). We performed a two-step qRT-PCR using SYBR Green Master Mix and the iQ5 System (Bio-Rad Laboratories, Munich, Germany). Glyceraldehyde-3-phosphate dehydrogenase (*Gapdh*) was used as reference gene. Oligonucleotide primers are listed in Supplementary Table 2. The amplification protocol was as follows: 95C for 3 min, followed by 40 cycles of 95C for 15 sec and 1 min at 60C, completed by a dissociation curve to identify false positive amplicons.

The relative expression level of each gene was calculated using the formula $2^{(-\Delta\Delta ct)}$.[16] Adult liver and fetal liver of ED 13.5 were used as standard controls and all samples were tested in triplicates. For each time point, the mean fold change of the expression level of at least three different liver specimens was calculated.

Protein Extraction and Western Blotting

Total protein was extracted from all specimens using sodium dodecyl sulfate (SDS) lysis buffer containing 0.5% SDS, 15 mM Tris-HCl (pH 6.8), 2.5% glycerol, 1 mM ethylene diamine-tetraacetic acid (EDTA) and proteinase inhibitor (Roche, Mannheim, Germany). After SDS-PAGE with equal amounts of protein (30 µg per lane), proteins were transferred onto nitrocellulose membranes (Whatman, Dassel, Germany) using a semidry blot system (Bio-Rad Laboratories, Munich, Germany). The membrane was blocked overnight at 4C in phosphate-buffered saline (PBS), pH 7.4, containing 5% dry milk powder. Primary antibodies, including goat anti-mouse Nope (R&D Systems, Minneapolis, MN), rabbit anti-mouse Cx26 (Invitrogen) and mouse anti-mouse β-actin (Sigma-Aldrich, Munich, Germany) were applied for 2 hr at room temperature. After extensive washing, membranes were incubated for 1 hr at room temperature with peroxidase-conjugated anti-goat (Sigma-Aldrich), anti-rabbit (Sigma-Aldrich), or anti-mouse IgG (Bio-Rad Laboratories), respectively. Immune complexes were detected using enhanced chemiluminescene (ECL) advance western blot substrate (Amersham, Braunschweig, Germany) according to the manufacturer's instructions. After detection, membranes were stripped using 0.2N NaOH for 10 min before application of the next primary antibody.

Immunohistochemistry

Liver tissue samples were fixed in 4% paraformaldehyde/sucrose, snap-frozen in ice-cold methyl butane and cryosections were prepared for immunohistochemistry. The following primary antibodies were used: Rat anti-mouse E-cadherin (TaKaRa, Otsu, Shiga, Japan), rat anti-mouse CK19 (TROMA, gift from R. Kemler, Freiburg, Germany), rat anti-mouse CD31 (BD Pharmingen, Heidelberg, Germany), goat anti-mouse Nope (R&D Systems), and rabbit anti-mouse Cx26 antibodies (Invitrogen). For details see Supplementary Table 3. These primary antibodies were detected through allophycocyanin (APC)-conjugated donkey anti-rat, Cy3-conjugated donkey anti-goat, Cy2-conjugated donkey anti-rabbit IgGs, respectively. Dipeptidyl peptidase (DPP) IV was detected using a fluorescein isothiocyanate (FITC)-conjugated rat anti-mouse antibody (BD Bioscience). Isotype controls were performed routinely to control for false positive reactions and background level. Nuclei were stained with 4´,6-diamidino-2-phenylindole (DAPI; Sigma-Aldrich). Fluorescence images were acquired using fluorescent microscope IX 81 (Olympus, Hamburg, Germany) and Cell P Analysis Software (AnalySIS, Soft Imaging System GmbH, Muenster, Germany).

Statistical Analysis

Unpaired *t* test analysis was performed to analyze for significant differences in gene expression using GraphPad Prism (version 6.07 for Windows, La Jolla, CA, www.graphpad.com). The presented *p* values are uncorrected and two-tailed and $\alpha < 0.05$ was considered as statistically significant (indicated as *, $\alpha < 0.01$ indicated as **, $\alpha < 0.001$ indicated as ***, and $\alpha < 0.0001$ indicated as ****).

Results

Expression of Nope and Cx26 During Physiological Liver Development

We quantified the expression levels of Nope and Cx26 by qRT-PCR at different stages of liver development to

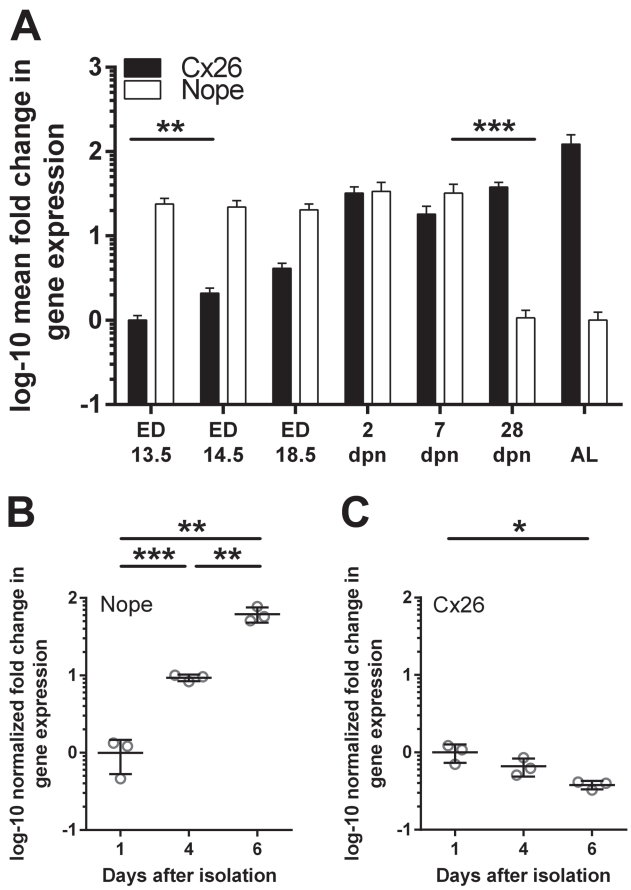

Figure 1. qRT-PCR of Nope and Cx26 during liver development (A) and in isolated primary murine hepatocytes (B and C). The expression levels of Nope (white bars) in the fetal liver remains constantly high until 7 dpn with a significant drop thereafter. The expression level of Cx26 (black bars) shows an inverse correlation. Cx26 is barely detectable in the fetal liver, but increases significantly after ED14.5 with a maximal expression level in the adult liver (A). In isolated primary murine hepatocytes cultivated on collagen I-coated plates, qRT-PCR analysis showed a significantly increasing expression level of Nope over time (B). The expression level of Cx26 showed a significant reduction over time (C). Expression levels were normalized to Gapdh. The relative mRNA expression is given as log 10-fold difference. Abbreviations: Nope, neighbor of Punc E11; qRT-PCR, quantitative real-time reverse transcription polymerase chain reaction; Cx, connexin; dpn, days postnatally; ED, embryonic day; AL, adult liver; *, $\alpha < 0.05$, **, $\alpha < 0.01$, and ***, $\alpha < 0.001$.

study physiological formation of hepatocyte polarity (Fig. 1A). During fetal liver development, Nope is constantly >20-fold higher expressed than in the adult liver. This high expression level is detectable until 1 wpn with a significant drop thereafter. At 4 wpn and thereafter, its expression remains barely detectable. For Cx26, however, the expression level shows an inverse correlation. In fetal liver tissue, the expression of Cx26 was barely detectable (ED13.5). However, a significant increase in Cx26 expression was measurable starting at ED14.5, with a further increase thereafter and a maximal expression level in the adult liver (Fig. 1A).

Nope Expression Is Induced in Isolated Primary Murine Hepatocytes in Cell Culture

To address changes in the expression of Nope after the loss of polarity in primary hepatocytes, isolated cells were cultivated on collagen I-coated plates and relative expression level of Nope was measured over time by qRT-PCR. The expression level of Nope increased significantly (9.3-fold by day 4 as compared with day 1; p=0.0001), and was even further enhanced by a 6.6-fold higher expression at day 6 versus day 4 after isolation (p=0.0028; 62-fold vs. day 1, p=0.0016; Fig. 1B). The expression level of Cx26 showed again an inverse trend with a significant reduction in expression over time (after 6 days 2.6-fold vs. day 1, p=0.0167; Fig. 1C).

Expression Level of Nope and Cx26 After BDL by qRT-PCR

We then made a comparative analysis of the differential expression pattern of Nope and Cx26 in adult liver with or without BDL as a model of cholestatic liver injury. The relative expression level of Nope was increasing as early as 1 day after BDL, reached significance at 2 days after BDL, and was finally reaching an 87-fold higher expression level versus adult liver after 1 week (p<0.001; Fig. 2A). Five weeks after BDL, the expression level was even 328-fold higher versus adult liver (p<0.001) which is even higher than the expression in the fetal liver (Fig. 2A).

The expression levels of Cx26 showed again an inverse trend. Cx26 is much higher expressed in the adult than in the fetal liver (259-fold vs. fetal liver), but was significantly reduced to a third of its expression level immediately after BDL compared with the adult liver although it remains much higher expressed than in the fetal liver (after 1 day 88-fold vs. fetal liver, p<0.001; Fig. 2B). The expression level of Cx26 was further reduced thereafter in comparison with the adult liver with a minimum expression level at 5 weeks after BDL (72.5-fold vs. fetal liver, p<0.001; Fig. 2B).

Validation of Nope and Cx26 During Fetal Liver Development and After BDL by Western Blotting

We then analyzed the protein levels of Nope and Cx26 in early and late stages of liver development including adult liver with or without BDL by Western blot analysis. Nope expression was detectable during all stages

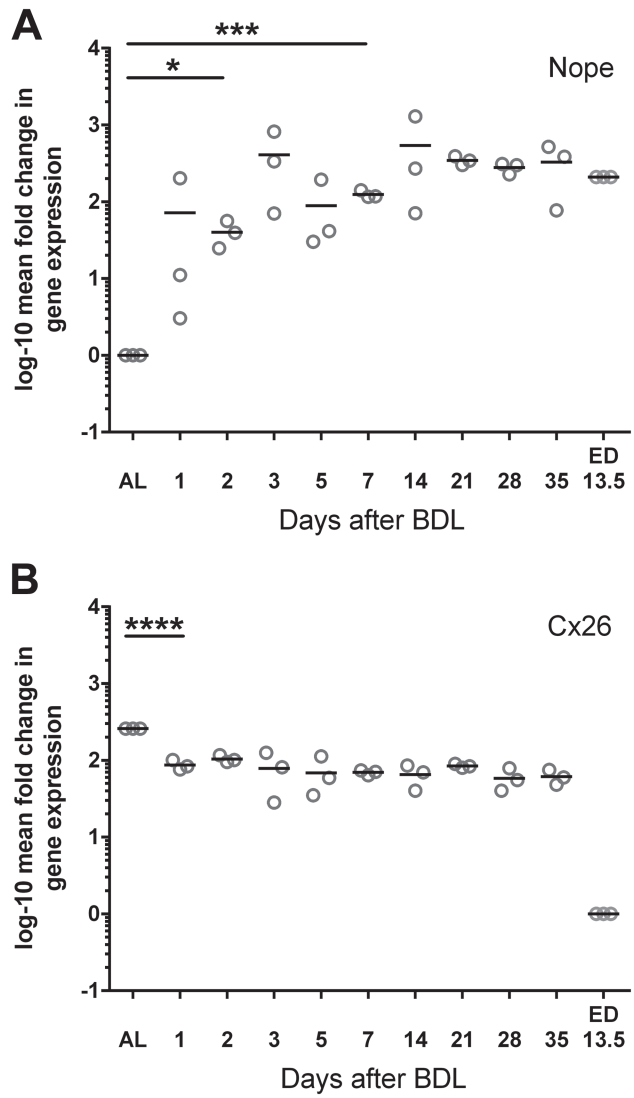

Figure 2. Temporal mRNA expression of Nope (A) and Cx26 (B) after BDL. The relative expression level of Nope was increasing as early as 1 day after BDL, reaching significance at 2 days after BDL and remained very high over time exceeding even the expression levels in fetal liver (A). Cx26 was significantly reduced to a third of its expression level immediately after BDL compared with the adult liver while it remains much higher expressed than in the fetal liver (B). Expression levels were normalized to *Gapdh*. The relative mRNA expression is given as log 10-fold difference. Each spot represents the mean of at least three different tissue samples from one animal to a total of three animals were analyzed for each time point. Abbreviations: Nope, neighbor of Punc E11; Cx, connexin; BDL, bile duct ligation; ED, embryonic day; AL, adult liver; *, $\alpha < 0.05$, **, $\alpha < 0.01$, ***, $\alpha < 0.001$, and ****, $\alpha < 0.0001$; Gapdh, glyceraldehyde-3-phosphate dehydrogenase.

of fetal and early postnatal liver development until 1 wpn (Fig. 3A). After 4 wpn and in the adult liver, however, the protein is not detectable any longer (Fig. 3A). Yet after BDL, Nope is again detectable as early as 72 hr after BDL and its expression level remains constantly elevated until 4 weeks after BDL (Fig. 3A).

In contrast, the protein expression of Cx26 is not detectable before ED18.5, but is high at 4 wpn and in the adult liver (Fig. 3B). After BDL, the expression level of Cx26 is markedly reduced at all analyzed time points (Fig. 3B) confirming the inverse correlation in the expression level of Nope and Cx26.

Distribution Pattern of Nope and Cx26 by Immunohistochemistry

Finally, the distribution pattern of Nope and Cx26 during liver development, in adult liver and after cholestatic liver injury was analyzed by immunohistochemistry.

At ED13.5, Nope is specifically expressed by early hepatoblasts with a fine granular staining in the cytoplasm and circumferentially on the whole plasma membrane while Cx26 is not yet detectable (Fig. 4A and B). At 1 wpn, Nope and Cx26 are both detectable on early hepatocytes. Although Nope has been directed to the sinusoidal membrane and is therefore in close proximity to CD31 positive sinusoidal endothelial cells (see arrows in Fig. 4D and F), Cx26 is heterogeneously distributed showing single patchy spots surrounding the whole hepatocyte with an irregular pattern (Fig. 4D and E). The merged picture visualizes therefore a partially overlapping expression of both proteins on the sinusoidal membrane at the postnatal stage (Fig. 4E, inlet). In the adult liver, Nope is not detectable on hepatocytes while Cx26 shows a punctate staining pattern on the membrane of hepatocytes (Fig. 4G and H). These costainings of Nope and Cx26 demonstrate the distinct spatial and temporal distribution pattern of these two markers during liver development revealing the physiological formation of hepatocyte polarity with early postnatal liver being the only time point at which both proteins are simultaneously expressed on hepatocytes.

Interestingly, we have found a coexpression of Nope and Cx26 also after BDL. Immunohistochemical staining for Nope after BDL reveals that expression of Nope is preferentially expressed on hepatocytes in zone 2 of the liver acinus (Fig. 5A). Costaining for Nope and E-cadherin, which marks hepatocytes in the periportal area, shows almost no overlap between the two proteins underlining the restriction of Nope to zone 2 (Fig. 5B). Costaining of Nope with CD31 as a marker of sinusoidal endothelial cells demonstrates that Nope is located in the neighboring sinusoidal membrane of hepatocytes (C). Finally, costaining with the bile canalicular marker protein DPPIV confirms that Nope is restricted to the sinusoidal membrane of hepatocytes (Fig. 5D) as described for postnatal liver.

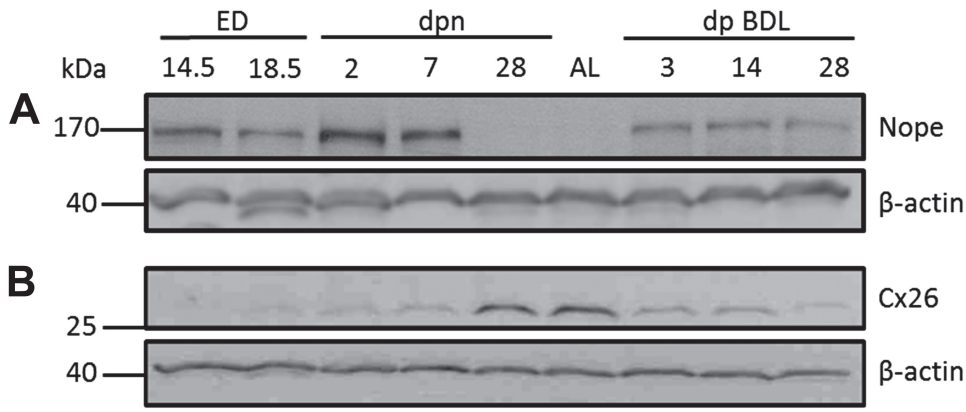

Figure 3. Western blot analysis of Nope and Cx26 during fetal liver development, in the adult liver and after BDL. Nope is detectable during liver development until 1 wpn (A). No expression is found after 4 wpn or in the adult liver (A). After BDL, however, Nope protein is again detectable (A). Cx26 protein is not detectable before ED18.5 (B). After 28 dpn and in the adult liver, Cx26 is strongly expressed (B). After BDL, the expression level of Cx26 is markedly reduced at all analyzed time points (B). β-actin was used as loading control. Abbreviations: Nope, neighbor of Punc E11; Cx, connexin; BDL, bile duct ligation; wpn, weeks postnatally; ED, embryonic day; AL, adult liver; dpn, days postnatally.

On the contrary, Cx26 remains detectable in the adult liver also after BDL though its distribution pattern changes over time which can be visualized by costainings with DPPIV (Figs. 6 and 8). In the adult liver, Cx26 and DPPIV display an overlapping expression pattern, indicating that Cx26 is restricted to the canalicular membrane of hepatocytes (Fig. 6A and B, and Fig. 8A and C). At 3 days after BDL, this expression pattern is almost unchanged (Fig. 6C and D). At 7 days after BDL, however, Cx26 is frequently also detectable as single spots on membranes negative for DPPIV, suggesting that it is partially translocated to the sinusoidal membrane of hepatocytes (Fig. 6E and F). At 28 days after BDL, Cx26 staining shows no longer its specific colocalization to the DPPIV-positive bile canalicular membrane of adult hepatocytes but is localized circumferentially on the whole membrane of hepatocytes (Fig. 6G and H).

Re-expression of Nope is detectable as early as 3 days after BDL on single hepatocytes which are also positive for Cx26 (Fig. 7A–D). At later time points after BDL, Nope remains restricted to the sinusoidal membrane, while Cx26 loses its restriction to the bile canalicular domain of hepatocytes, resulting in an increasing overlap of both proteins on the sinusoidal membranes. At 7 days after BDL, only single spots of Cx26 can be colocalized with Nope (Fig. 7F). At 28 days after BDL, Nope colocalizes with Cx26 on the majority of sinusoidal membranes of hepatocytes (Fig. 7H and Fig. 8F).

In general, immunohistochemical analysis confirms our quantitative expression data showing that Nope is expressed until early postnatal liver development and re-expressed shortly after BDL. Nope identifies not yet polarized hepatocytes in the early postnatal as well as depolarized hepatocytes in the biliary injured liver but is completely absent on polarized hepatocytes in the normal adult liver that are characterized through the restriction of Cx26 to their bile canalicular domain.

Discussion

In our previous work, we have demonstrated that Nope is a surface marker of murine fetal and adult liver stem/progenitor cells[3,5] as well as a specific and sensitive marker of hepatocellular carcinoma (HCC).[4] In our present study, we describe for the first time the expression of Nope on adult hepatocytes. Although the expression of Nope is physiologically downregulated in the postnatal period and barely detectable thereafter, the expression of Nope was significantly induced in adult hepatocytes after BDL. Interestingly, cholestatic liver injury has been recently described to come along with changes in hepatocyte polarity[2] and the expression of Nope after BDL is restricted to the sinusoidal membrane of adult hepatocytes and therefore resembles that of early postnatal hepatocytes which are in the final process of maturation and polarization. Indeed, Nope was also increasingly expressed on isolated adult primary hepatocytes after liver perfusion when they are challenged to regain their cell–cell contacts and polarity in cell culture conditions.

It is known that the establishment of polarity is not restricted to physiological liver development but occurs recurrently even thereafter.[17] Indeed, to fulfill their multiple functions in protein synthesis, metabolic homeostasis, and detoxification, it is essential for hepatocytes to sustain their unique organized polarity and to maintain the specified sinusoidal and bile canalicular spaces for the separation of blood from bile.[17] Therefore,

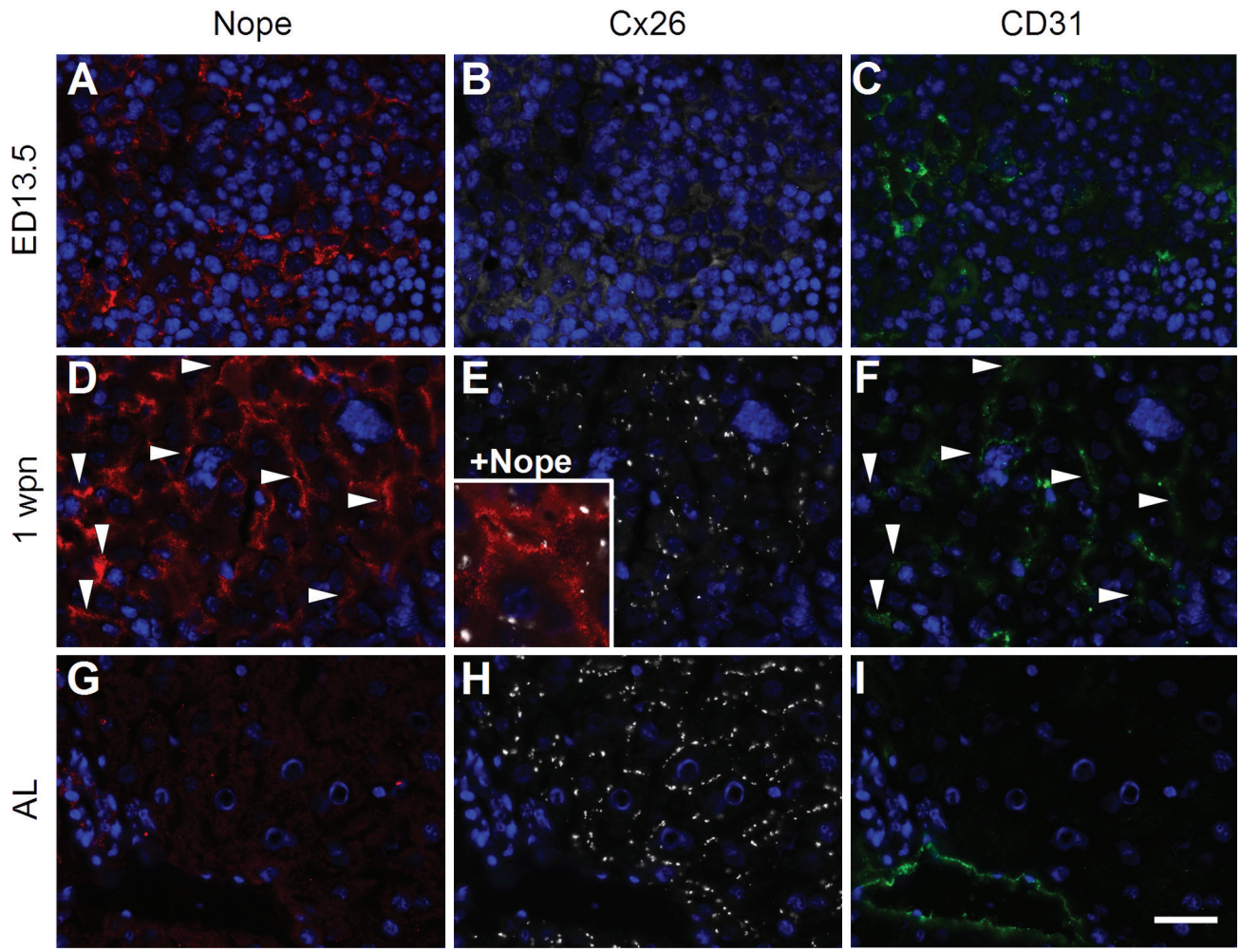

Figure 4. Immunohistochemistry of Nope, Cx26, and CD31 during liver development. Cryosections of early fetal (A, B, and C), early postnatal (D, E, and F) and adult murine livers (G, H, and I) were stained using antibodies for Nope (red; A, D, and G), Cx26 (white; B, E, and H) and CD31 (green: C, F, and I). Nuclei were stained with DAPI (blue). At ED13.5, Nope is specifically expressed by early hepatoblasts (A) while Cx26 is not yet detectable (B). CD31 detects early endothelial cells (C). At 1 wpn, Nope and Cx26 are both detectable on early postnatal hepatocytes. Nope has been directed to the sinusoidal membrane and is therefore in close proximity to CD31 positive sinusoidal endothelial cells (see arrows in D and F). Cx26 shows single patchy spots surrounding the whole hepatocyte with an irregular pattern (E). The merged picture visualizes therefore a partially overlapping expression of both proteins on the sinusoidal membrane (E, inlet). In the adult liver, Nope is not detectable in hepatocytes but weak expression is found in cholangiocytes (G). Cx26 shows a punctate staining pattern on hepatocytes (H) and CD31 is found on endothelial cells lining a large portal vein (I). Scale bar: 20 µm. Abbreviations: Nope, neighbor of Punc E11; Cx, connexin; DAPI, 6-diamidino-2-phenylindole; ED, embryonic day; AL, adult liver; wpn, weeks postnatally.

basolateral and apical domains have to be separated and sealed off by intercellular junctions which consist of tight junctions, anchoring junctions, and gap junctions.[18] Although gap junctions are not directly involved in epithelial polarity, they might contribute indirectly by supporting tight junction formation.[19] After finishing polarization, a specific and definitive Cx expression pattern is established in the adult liver, which is necessary for maintaining fully differentiated hepatocytes.[20] These express Cx26 specifically on their canalicular domain and Cx32, which is additionally expressed in cholangiocytes.[20,21]

We have therefore correlated our findings on Nope with the expression level and localization pattern of the gap junction protein Cx26 as a marker of hepatocyte polarity. Our findings reveal an inverse trend in the expression level of Nope and Cx26 along all analyzed stages of liver development including the adult liver with or without BDL and as such representing different stages of the formation of hepatocytic polarization (Schematic Fig. 9): In the fetal liver, not yet polarized hepatoblasts show high level of Nope expression with a ubiquitous localization on the plasma membrane while Cx26 is not yet detectable (Fig. 9A). Upon

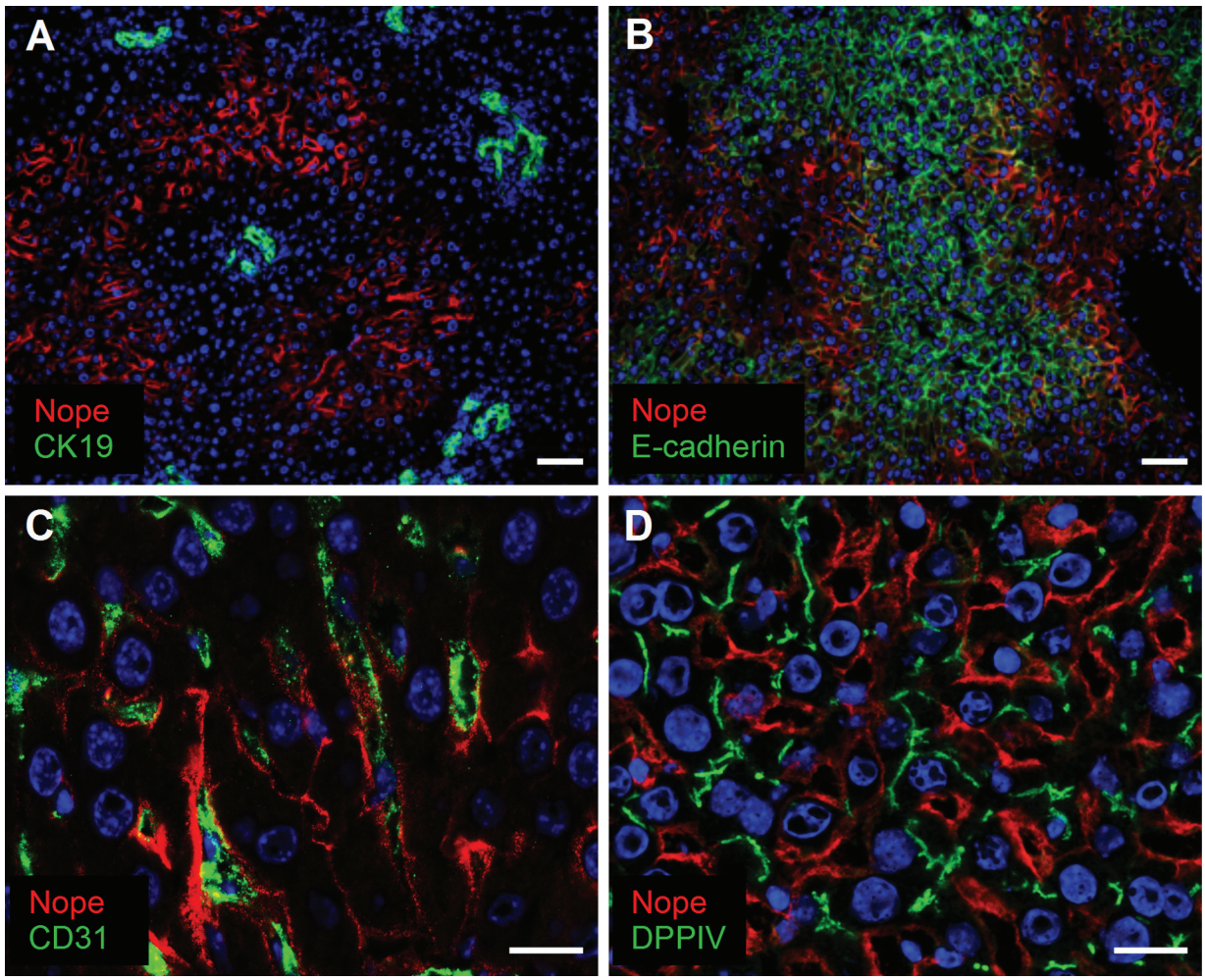

Figure 5. Immunohistochemistry of Nope after BDL. Cryosections of adult livers after BDL were stained using antibodies for Nope (red; A–D), CK19 (green; A), E-cadherin (green; B), CD31 (green; C), and DPPIV (green; D). Nuclei were stained with DAPI (blue). Costaining with CK19 reveals that expression of Nope is restricted to hepatocytes (A). E-cadherin stains periportally located hepatocytes and shows only a minimal overlap with Nope that stains preferentially hepatocytes in zone 2 of the liver acinus (B). Costaining of Nope with CD31 as a marker of sinusoidal endothelial cells demonstrates that Nope is located in the neighboring sinusoidal membrane of hepatocytes (C). The bile canalicular marker DPPIV complements the sinusoidal membrane localization of Nope on hepatocytes after BDL (D). Scale bar A and B: 50 μm. Scale bar C and D: 20 μm. Abbreviations: Nope, neighbor of Punc E11; BDL, bile duct ligation; DAPI, 6-diamidino-2-phenylindole; DPPIV, dipeptidyl peptidase IV.

initiation of polarization in the early postnatal liver, Nope is directed to the sinusoidal membrane while the expression level of Cx26 is increasing with a patchy distribution over the whole membrane of early postnatal hepatocytes (Fig. 9B). In the adult liver, Nope is not expressed any longer on fully differentiated and polarized hepatocytes and Cx26 is highly expressed but restricted to the bile canalicular domain (Fig. 9C). After BDL, the expression level and pattern of Nope and Cx26 resemble that of early postnatal hepatocytes that are initiating polarization (Fig. 9D).

We hypothesize that this inverse correlation and expression pattern may be found in various other stages, in which polarization of hepatocytes is lost or reorganized, for example, in neoplastic hepatocytes that are known to lose their original polarization.[22] Indeed, it has been shown that bile canalicular proteins in general are mislocalized in HCC and can be found on the entire surface membrane of neoplastic cells.[21] Specifically, Cx26 has been described to be downregulated in HCC by methylation.[23] In fact, dissection of the HCC morphology demonstrated defects in the distribution of bile canalicular proteins even in preneoplastic hepatocytes.[21] On the contrary, Nope has been identified in previous studies as an oncological surface marker for murine and human alfa-fetoprotein (Afp)-positive and Afp-negative HCC but not in preneoplastic stages or in normal liver tissue.[4] This

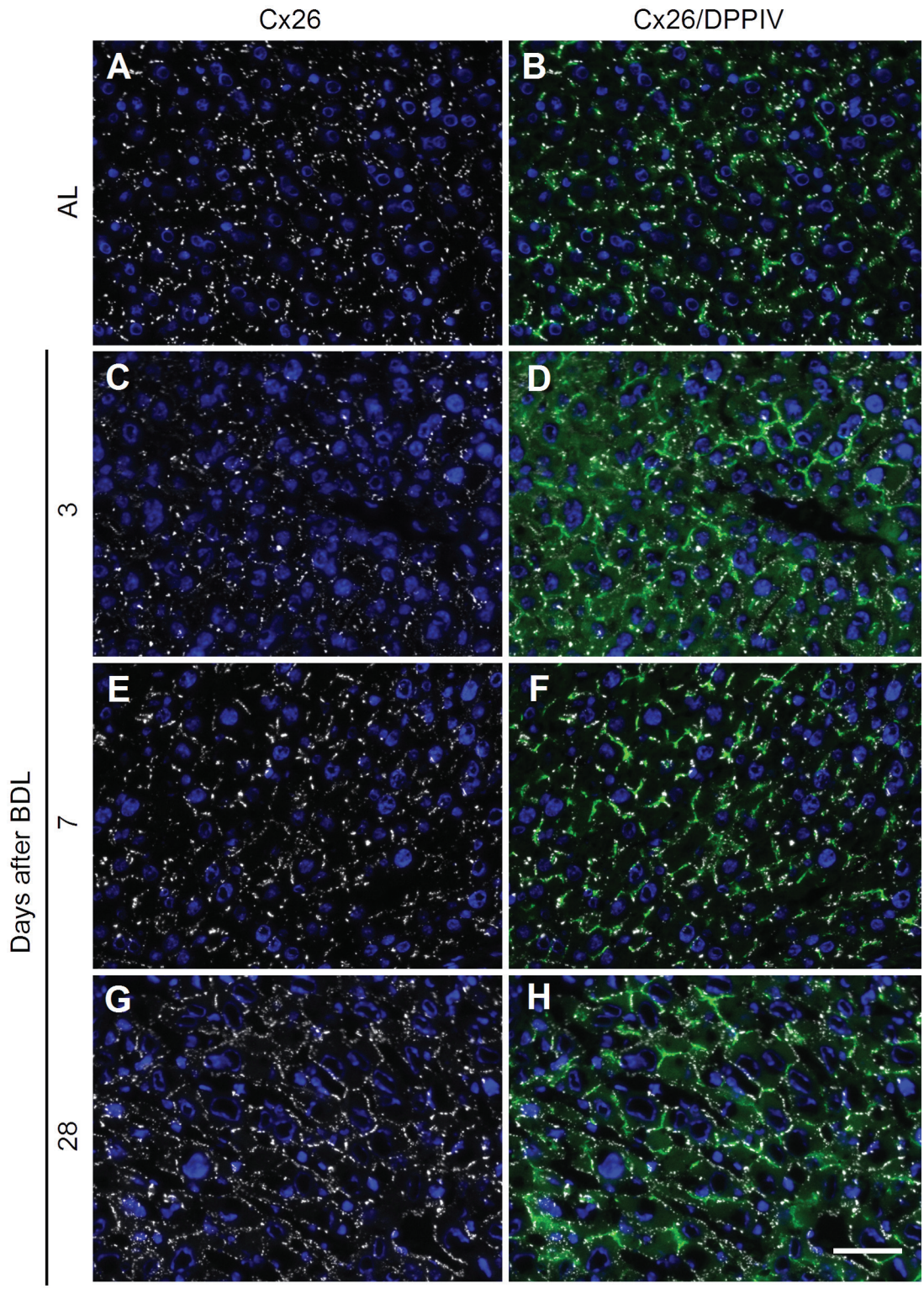

Figure 6. Expression pattern of Cx26 and DPPIV in adult liver with or without BDL. Cryosections of adult liver (A and B) or 3, 7, and 28 days after BDL (C–H) were costained using antibodies for Cx26 (white; A–H) and DPPIV (green; B, D, F, and H). Nuclei were stained with DAPI (blue). In the adult liver, Cx26 protein is restricted to the canalicular membrane (A) as indicated by the colocalization with DPPIV (B). This expression pattern changes after BDL. At 3 days after BDL, Cx26 is still mainly colocalized with DPPIV (C and D). At 7 days after BDL, Cx26 is frequently also detectable on the sinusoidal membrane of hepatocytes without overlapping DPPIV staining (E and F). At 28 days after BDL, Cx26 staining has lost its restriction to the DPPIV-positive bile canalicular membrane but is localized circumferentially on the whole membrane of hepatocytes (G and H). Scale bar: 50 µm. Abbreviations: DPPIV, dipeptidyl peptidase IV; Cx, connexin; BDL, bile duct ligation; AL, adult liver; DAPI, 6-diamidino-2-phenylindole.

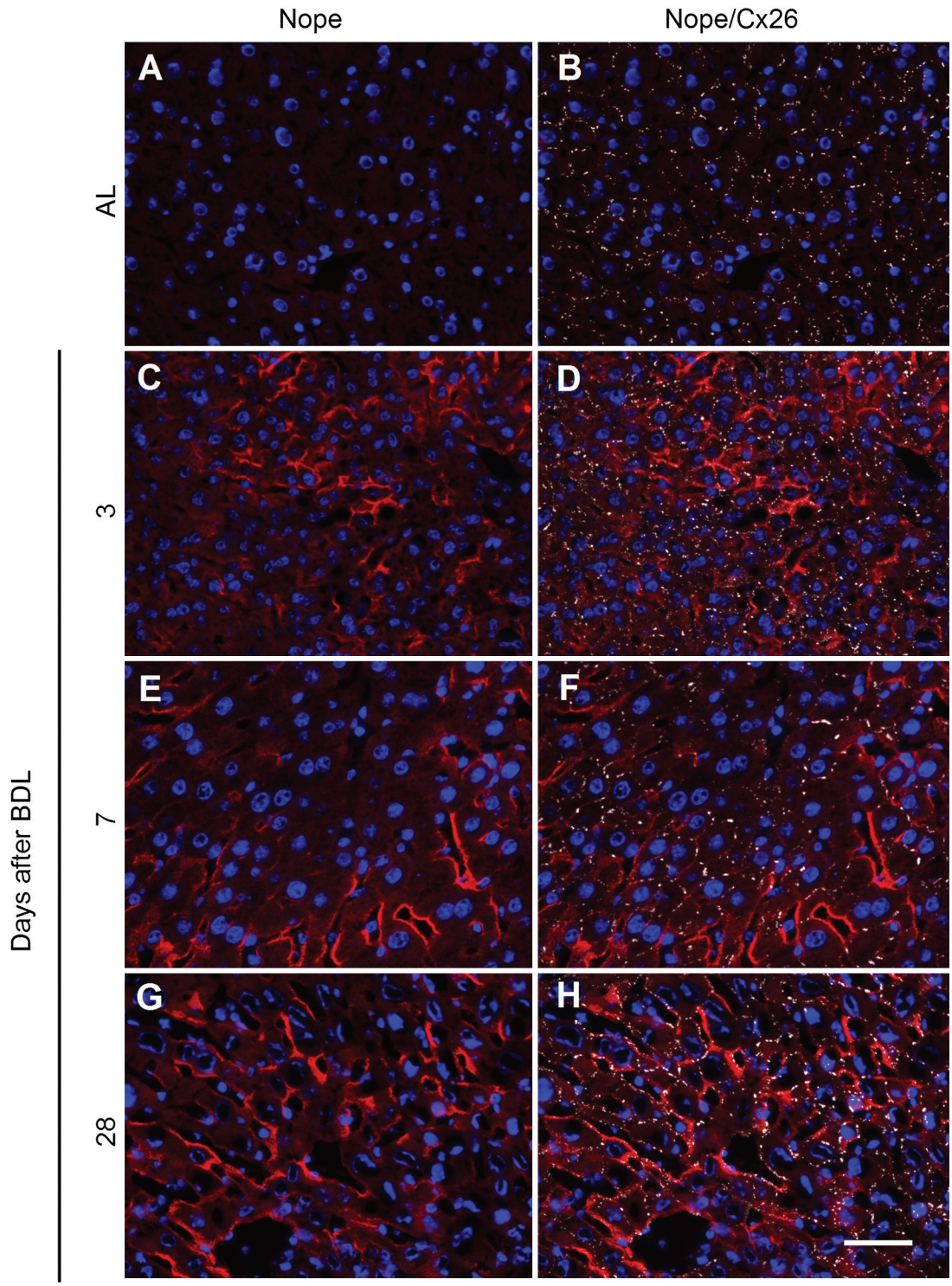

Figure 7. Expression pattern of Cx26 and Nope in adult liver with or without BDL. Cryosections of adult liver (A and B) or 3, 7, and 28 days after BDL (C–H) were costained using antibodies for Nope (red; A–H) and Cx26 (white; B, D, F, and H). Nuclei were stained with DAPI (blue). In the adult liver, Nope is not detectable (A) and Cx26 is restricted to the bile canalicular membrane of hepatocytes (B). At 3 days after BDL, Nope expression is detectable at the sinusoidal membrane of single hepatocytes (C) which are positive for Cx26 but rarely overlapping (D). At 7 days after BDL, Nope expression is increased and single spots of Cx26 colocalize with Nope (E and F). At 28 days after BDL, Nope colocalizes with Cx26 on the majority of sinusoidal membranes of hepatocytes (G and H). Scale bar: 50 µm. Abbreviations: Nope, neighbor of Punc E11; Cx, connexin; BDL, bile duct ligation; AL, adult liver; DAPI, 6-diamidino-2-phenylindole.

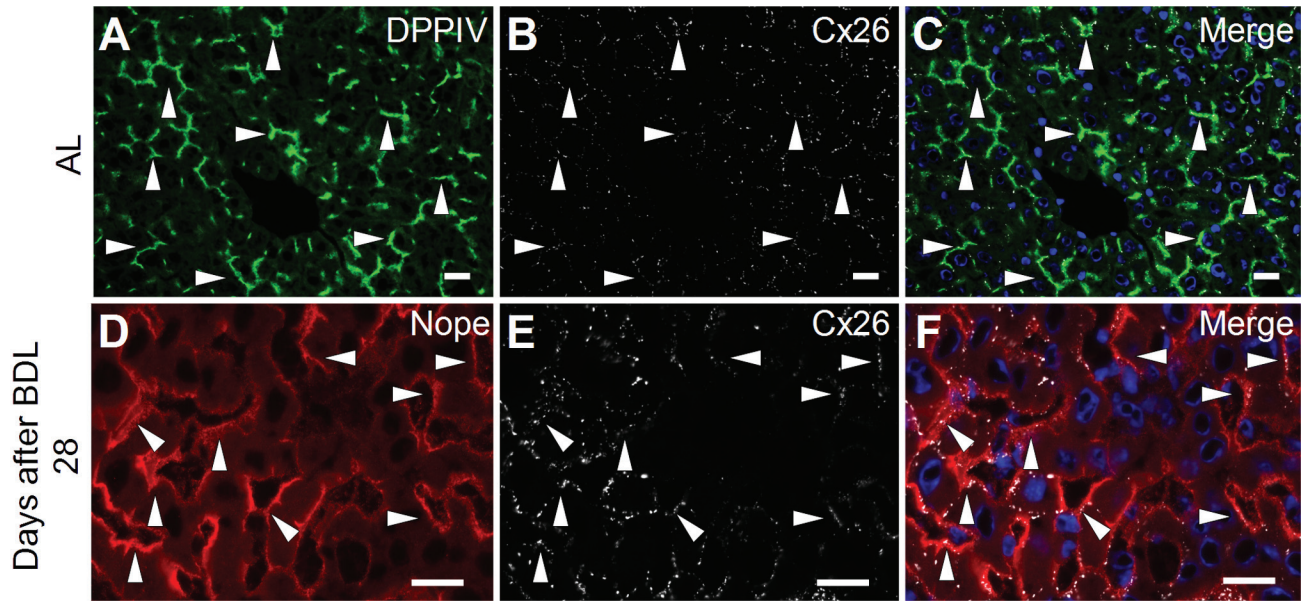

Figure 8. Changes in the expression pattern of Cx26 after bile duct ligation. Cryosections of adult liver (A, B, and C) and 28 days after BDL (D, E, and F) were costained using antibodies for DPPIV (green; A and C), Cx26 (white; B, C, E, and F) and Nope (red; D and F). Nuclei were stained with DAPI (blue). While DPPIV and Cx26 are both restricted to the bile canalicular membrane in the adult liver (A–C), Cx26 expression loses its specific localization after BDL and shows a circumferential expression pattern on hepatocytes (E). This results in an overlapping expression with Nope that is upregulated after BDL but remains restricted to the sinusoidal membranes of hepatocytes (D and F). Scale bar: 20 µm. Abbreviations: Nope, neighbor of Punc E11; Cx, connexin; BDL, bile duct ligation; AL, adult liver; DPPIV, dipeptidyl peptidase IV; DAPI, 6-diamidino-2-phenylindole.

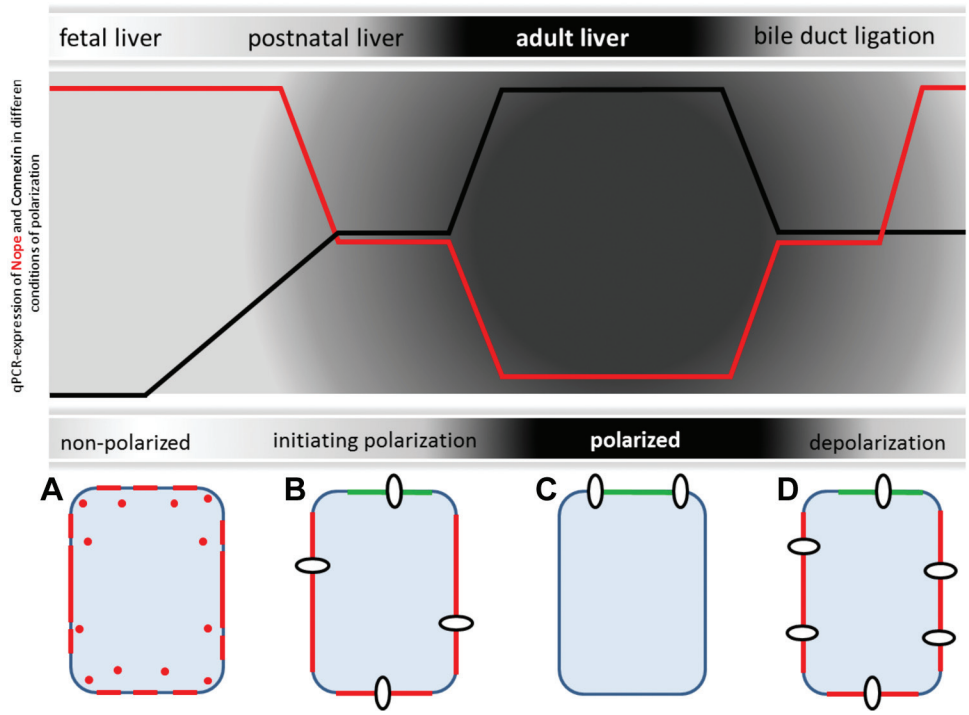

(continued)

Figure 9. Schematic representation of Nope and Cx26 during polarization and depolarization of hepatocytes. In the fetal liver, not yet polarized hepatoblasts show high level of Nope (red) expression with a circular membrane staining while Cx26 is not yet detectable (9A). Upon initial polarization in the postnatal liver, Nope is directed to the sinusoidal membrane and DPPIV (green) identifies the canalicular membrane while the expression level of Cx26 (white circles) is increasing with a patchy distribution over the whole membrane of early postnatal hepatocytes (9B). In the adult liver, Nope is not expressed any longer on fully differentiated and polarized hepatocytes and Cx26 is highly expressed but restricted to the canalicular domain (9C). After BDL, the expression level and pattern of Nope and Cx26 resemble that of early postnatal hepatocytes that are initiating polarization (9D). Abbreviations: Nope, neighbor of Punc E11; Cx, connexin; DPPIV, dipeptidyl peptidase IV; BDL, bile duct ligation; AL, adult liver; qRT-PCR, quantitative real-time reverse transcription polymerase chain reaction.

has been recently confirmed in diethylnitrosamine (DEN)-induced murine HCC.[24]

Whether the expression of Nope is essential for hepatocytic polarization or is just triggered by similar mechanisms remains elusive, since the function of Nope is unknown and can only be postulated in analogy to its reported family members in the deleted in colorectal cancer (DCC) subgroup of the immunoglobulin superfamily such as Punc, Dcc, and Neogenin. Functionally, Punc has been correlated with proliferating cells, whereas the expression of Dcc and Neogenin is generally associated with cells starting to differentiate.[25] Particularly Neogenin is reported to be expressed during the transition of undifferentiated into differentiated cell types.[26] However, Nope is so far the only Dcc subfamily member to be expressed in the liver during embryogenesis.[3,27,28] Dcc and Neogenin are both expressed in the developing central nervous system, urogenital, and cartilage, only Neogenin is additionally found in the developing gut, lung, and heart.[27] To fully understand the functional role of Nope in hepatocytic polarization, we are currently developing a conditional knock out mouse model.

In a recent review on cholestatic liver diseases, Jansen et al. pointed out that disease stage-defining biomarkers are still lacking.[1] As cholestatic liver injury induces changes in hepatocyte polarity, Nope might be a marker of depolarized hepatocytes in cholestatic liver injury, for example, in primary sclerosing cholangitis. We here demonstrate that the expression of Nope is highly sensitive to biliary injury of the liver parenchyma, being detectable as early as one day after BDL by qRT-PCR with increasing levels over time, indicating a time and dose-dependent sensitivity. Interestingly, Nope identifies a homogeneous population of hepatocytic cells in the fetal or postnatal liver and in murine HCC that ubiquitously show the same staining pattern. After BDL, however, Nope identifies only a subset of depolarized adult hepatocytes within the liver lobule that cannot be identified or differentiated from the surrounding hepatocytes by any other marker (data not shown). Therefore, Nope might provide a valuable tool to detect biliary injury at asymptotic or symptom-poor stages preceding overt cholestasis or severe stages in which hepatocytes are affected by the underlying cholestatic liver disease leading to liver cirrhosis. Its usefulness as a biomarker in cholestatic liver disease for the classification of the course of disease or monitoring of therapy will have to be assessed in additional investigations including detection in long-term, compensatory regeneration models.

In conclusion, we here describe for the first time the expression of the oncofetal stem/progenitor cell marker Nope on adult hepatocytes. Nope identifies a subset of depolarized adult hepatocytes after cholestatic liver injury resembling early postnatal hepatocytes beginning to polarize. We therefore postulate that Nope might be a valuable histochemical biomarker allowing stage-specific stratifications or therapeutic monitoring in cholestatic liver diseases.

Acknowledgments

We are grateful to Gisela Holz and Elisabeth Konze for excellent technical assistance and Robert Kemler, Freiburg, Germany, for TROMA antibody.

Competing Interests

The author(s) declared no potential conflicts of interest with respect to the research, authorship, and/or publication of this article.

Author Contributions

All authors have contributed to this article as follows: study concept and design (AB, DN), bile duct ligation (AB), acquisition of data (AB, SZ), analysis and interpretation of data (AB, SZ, VM, DN), statistical analysis (SZ), material support and critical revision of the manuscript for important intellectual content (VK, SS), obtained funding (TG, DN), and drafting of the manuscript (AB, SZ, DN).

Funding

The author(s) disclosed receipt of the following financial support for the research, authorship, and/or publication of this article: This research project was supported by the Wilhelm-Doerenkamp Foundation, Cologne, and the Medical Faculty of the University of Cologne.

ORCID iD

V Kondylis https://orcid.org/0000-0002-6970-8731

Literature Cited

1. Jansen PL, Ghallab A, Vartak N, Reif R, Schaap FG, Hampe J, Hengstler JG. The ascending pathophysiology of cholestatic liver disease. Hepatology. 2017;65(2):722–38. doi:10.1002/hep.28965.
2. Gissen P, Arias IM. Structural and functional hepatocyte polarity and liver disease. J Hepatol. 2015;63(4):1023–37. doi:10.1016/j.jhep.2015.06.015.
3. Nierhoff D, Levoci L, Schulte S, Goeser T, Rogler LE, Shafritz DA. New cell surface markers for murine fetal hepatic stem cells identified through high density complementary DNA microarrays. Hepatology. 2007;46(2):535–47. doi:10.1002/hep.21721.
4. Marquardt JU, Quasdorff M, Varnholt H, Curth HM, Mesghenna S, Protzer U, Goeser T, Nierhoff D. Neighbor of Punc E11, a novel oncofetal marker for hepatocellular carcinoma. Int J Cancer. 2011;128(10):2353–63. doi:10.1002/ijc.25567.
5. Schievenbusch S, Sauer E, Curth HM, Schulte S, Demir M, Toex U, Goeser T, Nierhoff D. Neighbor of Punc E 11: expression pattern of the new hepatic stem/progenitor cell marker during murine liver development. Stem Cells Dev. 2012;21(14):2656–66. doi:10.1089/scd.2011.0579.
6. Spray DCS, Sáez JC, Hertzberg EL, Dermietzel R. Gap junctions in liver: composition function and regulation. In: Arias IMB, Boyer JL, Fausto N, Jakoby WB, Schachter DA, & Shafrits DA, editors. The liver: biology and pathobiology. 3rd ed. New York: Raven Press; 1994. p. 951–67.
7. Neveu MJ, Hully JR, Babcock KL, Vaughan J, Hertzberg EL, Nicholson BJ, Paul DL, Pitot HC. Proliferation-associated differences in the spatial and temporal expression of gap junction genes in rat liver. Hepatology. 1995;22(1):202–12.
8. Iwai M, Harada Y, Muramatsu A, Tanaka S, Mori T, Okanoue T, Katoh F, Ohkusa T, Kashima K. Development of gap junctional channels and intercellular communication in rat liver during ontogenesis. J Hepatol. 2000;32(1):11–8.
9. Vinken M, Doktorova T, Decrock E, Leybaert L, Vanhaecke T, Rogiers V. Gap junctional intercellular communication as a target for liver toxicity and carcinogenicity. Crit Rev Biochem Mol Biol. 2009;44(4):201–22. doi:10.1080/10409230903061215.
10. Vinken M, Henkens T, De Rop E, Fraczek J, Vanhaecke T, Rogiers V. Biology and pathobiology of gap junctional channels in hepatocytes. Hepatology. 2008;47(3):1077–88. doi:10.1002/hep.22049.
11. Odin P, Obrink B. Dynamic expression of the cell adhesion molecule cell-CAM 105 in fetal and regenerating rat liver. Exp Cell Res. 1986;164(1):103–14.
12. Odin P, Obrink B. The cell-surface expression of the cell adhesion molecule cellCAM 105 in rat fetal tissues and regenerating liver. Exp Cell Res. 1988;179(1):89–103.
13. Bartles JR, Hubbard AL. Preservation of hepatocyte plasma membrane domains during cell division in situ in regenerating rat liver. Dev Biol. 1986;118(1):286–95.
14. Fallon MB, Nathanson MH, Mennone A, Saez JC, Burgstahler AD, Anderson JM. Altered expression and function of hepatocyte gap junctions after common bile duct ligation in the rat. Am J Physiol. 1995;268(5 Pt 1):C1186–94.
15. Kondylis V, Polykratis A, Ehlken H, Ochoa-Callejero L, Straub BK, Krishna-Subramanian S, Van TM, Curth HM, Heise N, Weih F, Klein U, Schirmacher P, Kelliher M, Pasparakis M. NEMO prevents steatohepatitis and hepatocellular carcinoma by inhibiting RIPK1 kinase activity-mediated hepatocyte apoptosis. Cancer Cell. 2015;28(5):582–98. doi:10.1016/j.ccell.2015.10.001.
16. Livak KJ, Schmittgen TD. Analysis of relative gene expression data using real-time quantitative PCR and the 2(-Delta Delta C(T)) Method. Methods. 2001;25(4):402–8. doi:10.1006/meth.2001.1262.
17. Treyer A, Musch A. Hepatocyte polarity. Compr Physiol. 2013;3(1):243–87. doi:10.1002/cphy.c120009.
18. Musch A. The unique polarity phenotype of hepatocytes. Exp Cell Res. 2014;328(2):276–83. doi:10.1016/j.yexcr.2014.06.006.
19. Kojima T, Murata M, Go M, Spray DC, Sawada N. Connexins induce and maintain tight junctions in epithelial cells. J Membr Biol. 2007;217(1–3):13–9. doi:10.1007/s00232-007-9021-4.
20. Crespo Yanguas S, Willebrords J, Maes M, da Silva TC, Veloso Alves Pereira I, Cogliati B, Zaidan Dagli ML, Vinken M. Connexins and pannexins in liver damage. EXCLI J. 2016;15:177–86. doi:10.17179/excli2016-119.
21. Bode HP, Wang L, Cassio D, Leite MF, St-Pierre MV, Hirata K, Okazaki K, Sears ML, Meda P, Nathanson MH, Dufour JF. Expression and regulation of gap junctions in rat cholangiocytes. Hepatology. 2002;36(3):631–40. doi:10.1053/jhep.2002.35274.
22. Goodman ZD. Neoplasms of the liver. Mod Pathol. 2007;20(Suppl 1):S49–60. doi:10.1038/modpathol.3800682.
23. Shimizu K, Onishi M, Sugata E, Sokuza Y, Mori C, Nishikawa T, Honoki K, Tsujiuchi T. Disturbance of DNA methylation patterns in the early phase of hepatocarcinogenesis induced by a choline-deficient L-amino acid-defined diet in rats. Cancer Sci. 2007;98(9):1318–22. doi:10.1111/j.1349-7006.2007.00564.x.
24. Kim YH, Kwak KA, Kang JS. Expression of neighbor of Punc E11 in hepatocarcinogenesis induced by diethylnitrosamine. Oncol Rep. 2014;32(3):1043–9. doi:10.3892/or.2014.3285.
25. Salbaum JM, Kappen C. Cloning and expression of nope, a new mouse gene of the immunoglobulin superfamily related to guidance receptors. Genomics. 2000;64(1):15–23. doi:10.1006/geno.2000.6114.
26. Vielmetter J, Chen XN, Miskevich F, Lane RP, Yamakawa K, Korenberg JR, Dreyer WJ.Molecular characterization of human neogenin, a DCC-related protein,

and the mapping of its gene (NEO1) to chromosomal position 15q22.3-q23. Genomics. 1997;41(3):414–21. doi:10.1006/geno.1997.4688.

27. Gad JM, Keeling SL, Wilks AF, Tan SS, Cooper HM. The expression patterns of guidance receptors, DCC and Neogenin, are spatially and temporally distinct throughout mouse embryogenesis. Dev Biol. 1997;192(2):258–73. doi:10.1006/dbio.1997.8756.
28. Fitzgerald DP, Seaman C, Cooper HM. Localization of Neogenin protein during morphogenesis in the mouse embryo. Dev Dyn. 2006;235(6):1720–5. doi:10.1002/dvdy.20744.